

of the hepatocytes, bulging of the regenerated hepatocytes and proliferation of atypical hepatocytes and oncocytes.

Immunohistochemistry

Paraffin-embedded specimens were sliced into 3 to 4 μm sections, deparaffinized, and subjected to heat-induced epitope retrieval at 98°C for 40 minutes. After blocking endogenous peroxidase activity using 3% hydrogen peroxide, the slide was incubated with appropriately diluted primary antibodies. Antihuman CD4, antihuman CD8 and antihuman CD14 mouse monoclonal antibodies were used to evaluate the immunoreactivity of HCC using a DAKO EnVision+™ kit, as described in the manufacturer's instructions.

We semiquantitatively analyzed tumor tissues by assigning a score to the severity of CD4-positive and CD8-positive lymphocyte infiltration in the tumor tissue (0 for none, 1 for mild, 2 for moderate, and 3 for severe).

Statistical analysis

Fisher exact probability test was used to compare categorical variables and the Mann-Whitney *U* test was used to compare continuous variables; a *P* value of less than 0.05 was considered statistically significant. The TTR survival curve was analyzed using the Kaplan-Meier curve and compared by the log-rank test. Univariate Cox regression analysis was conducted to identify TTR predictors out of clinical and biologic parameters [sex, age, *IL-28B* genotype, therapy, platelet count, alanine aminotransferase (ALT), γ -GTP, albumin, prothrombin activity, bilirubin, Child-Pugh class, history of IFN therapy, AFP, and des- γ -carboxy prothrombin (DCP)] and tumor factors (size and number).

Multivariate analysis was conducted using the Cox regression model with backward elimination (27). The significance level for removing a factor from the model was set to 0.05. A bootstrap technique was applied to confirm the choice of variables (27). One thousand bootstrap samples were generated using resampling with replacement and Cox regression analysis with backward elimination was applied to each sample. The percentage of samples (from the total of 1,000) for which each variable was included in the model was calculated. In multivariate analysis, we evaluated two models that contained either Child-Pugh class or its components to avoid multicollinearity. Data analysis was conducted with R software. We used functions from the Regression Modeling Strategies library for validation with the bootstrap technique (28).

Results

Patient characteristics and *IL-28B* genotype frequency

We genotyped 183 patients with HCC for the *IL-28B* rs8099917 TT, TG, and GG genotypes and observed respective proportions of 67.8% (124 of 183), 30.6% (56 of 183), and 1.6% (3 of 183), which is a similar distribution to that observed in several Japanese studies of patients with CHC (13, 14, 29, 30). Although the prevalence of the TG/GG genotype was higher than that of the general

population (12%–16%; refs. 12, 31, 32), there was no significant difference between our result and that of HCV-infected patients in a previous study. There was also no significant difference in clinical variables between the TT and TG/GG genotypes (Table 1).

We next genotyped 160 of 183 cases for rs12979860 and our findings were largely in concordance with those of rs8099917, with the exception of 1 case (0.6%). The haplotype of the case showed that rs8099917 was TT and rs12979860 was CT suggesting that these 2 loci are in a haplotype block with a high level of linkage disequilibrium, as previously reported (13, 30). Genotype distribution analysis showed that rs8099917 was in Hardy-Weinberg equilibrium, so we selected it for further investigation.

During the median follow-up period of 2.5 years (range, 0.3–7.2 years), 118 of 183 patients developed HCC recurrence. Local tumor progression was seen in 13 patients treated by RFA and in only 1 patient treated by resection. The local tumor progression rate and distant recurrence rate were 2.6% and 21.2% in the first year and 8.3% and 54.2% within 2.5 years, respectively. These results are comparable with previous reports by others (33, 34). The type of recurrence was also comparable between *IL-28B* genotype groups.

Associations between the *IL-28B* genotype and HCC clinical outcome

HCC TTR was also analyzed using multivariate Cox regression analysis using 15 clinical parameters and the *IL-28B* genotype. With a significance level of 0.05 for removing a variable in a Cox regression with backward elimination, the *IL-28B* genotype was selected as the final model (Table 2). To confirm this decision, a bootstrapping technique was applied. The percentages of inclusion among the 1,000 samples created by the bootstrapping technique for variables are shown in Table 2. The percentage of inclusion for the *IL-28B* genotype was 80.4%. Frequencies of another variable were lower than 40%. The bootstrap procedure result confirmed the variables chosen for the final model.

In univariate Cox regression analyses, the *IL-28B* genotype was associated with HCC recurrence (Table 2). The TTR survival curve was analyzed using the Kaplan-Meier curve and log-rank test (Fig. 1), and patients with the *IL-28B* TT genotype showed a significantly shorter median TTR (1.61 years) than those with the *IL-28B* TG/GG genotype (2.58 years; *P* = 0.007).

Histologic analysis of noncancerous liver tissues of *IL-28B* TT and TG/GG genotypes

To clarify the molecular mechanism influencing HCC recurrence, we histologically analyzed 141 noncancerous liver tissues according to previously published criteria (Table 3; ref. 26). The mean score of the degree of inflammatory cell infiltration in the periportal area was significantly higher in TT genotype patients (2.804) than TG/GG genotype patients (2.513; *P* = 0.025); the degree of inflammatory cell infiltration in the intralobular area was also

Table 2. Cox regression analysis and relative frequency of variables inclusion with $P < 0.05$ (in 1,000 bootstrap samples)

Variables	Univariate		Multivariate		Frequency (%)
	HR (95% CI)	P	HR (95%CI)	P	
IL-28B allele: major vs. minor	2.674 (1.161–2.627)	0.007	2.674 (1.161–2.627)	0.007	80.4
Tumor size, mm: >20 vs. ≤20	1.303 (0.881–1.880)	0.193			39.8
AFP, ng/mL: >20 vs. ≤20	1.674 (0.948–1.968)	0.094			33.2
γ-GTP, IU/L: >50 vs. ≤50	1.188 (0.865–1.804)	0.235			32.8
Therapy: RFA vs. resection	1.218 (0.826–2.266)	0.223			31.6
DCP, AU/L: >40 vs. ≤40	1.524 (0.920–1.945)	0.127			27.4
ALT, IU/L: >40 vs. ≤40	0.277 (0.721–1.544)	0.782			23.6
Child–Pugh class: A vs. B	0.025 (0.653–1.515)	0.980			19.2
Period of therapy: 2000-05 vs. 2006-12	0.886 (0.818–1.701)	0.375			15.8
History of IFN therapy: yes vs. no	0.570 (0.771–1.605)	0.569			15.8
Sex: male vs. female	0.108 (0.697–1.496)	0.914			14.6
Tumor number: solitary vs. 2-3	0.263 (0.845–1.857)	0.263			13.4
Platelet count ($\times 10^4/\text{mm}^3$): >10 vs. ≤10	0.118 (0.680–1.407)	0.906			12.6
Age: per 1 y	0.621 (0.986–1.028)	0.534			8.4

higher in the TT genotype (2.522) than the TG/GG genotype (2.308), although this did not reach statistical significance ($P = 0.08$). Furthermore, the mean score of the degree of hepatocyte anisocytosis was significantly higher in the TT genotype (1.891) than the TG/GG genotype (1.385; $P = 0.024$). Anisocytosis is characterized by variability of cell size with focal dysplastic change and indicates irregular regeneration of hepatocytes. The irregular regeneration score was higher in the TT genotype (2.207) than the TG/GG genotype (1.795), albeit not significantly ($P = 0.105$).

IL-28B TT and TG/GG genotype gene expression profiles in the noncancerous liver

We next compared the gene expression profile of HCC tissues and noncancerous liver tissues of both the IL-28B TT

and IL-28B TG/GG genotype. Ten patients with HCC were selected from each IL-28B genotype and their gene expression was determined using Affymetrix genechip analysis (Supplementary Table S1). We recently reported that expression of hepatic ISGs is downregulated in individuals with the IL-28B TT genotype, whereas the expression of other immune response-related genes was shown to be upregulated (13). Therefore, to validate our expression data, we compared the expression of ISGs and other immune response-related genes in the present study with that of the previous study. We analyzed the expression data of 20 patients from the current study in addition to another series of 91 patients with CHC from our previous study.

One-way hierarchical clustering using 28 representative ISGs showed that patients with the IL-28B TG/GG genotype

Figure 1. Kaplan–Meier curves of early and overall TTR in relation to IL-28B genotype. The patients with the IL-28B TT genotype showed a significantly shorter median TTR (1.61 years) than those with the IL-28B TG/GG genotype (2.58 years; $P = 0.007$).

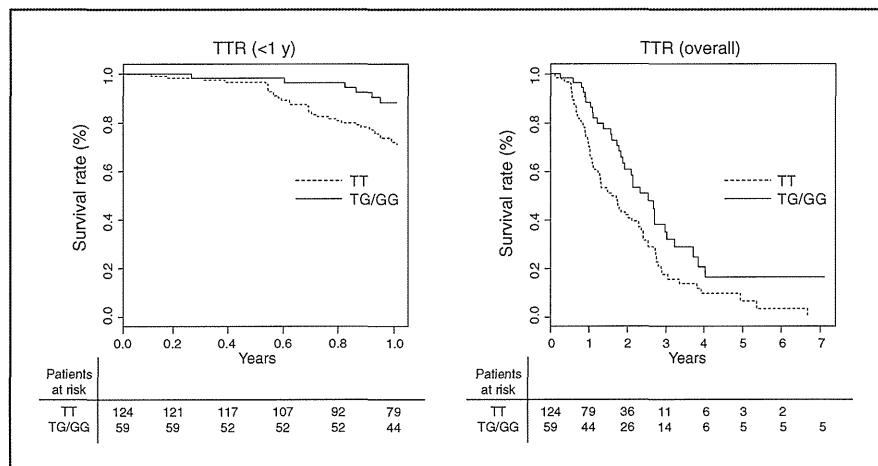


Table 3. Comparison of liver histology between *IL-28B* major and minor genotypes

Variable	<i>IL-28B</i> TT genotype (n = 92)	<i>IL-28</i> TG/GG genotype (n = 39)	P value
Score of inflammatory cell infiltration			
Periportal	2.804	2.513	0.032
Intralobular	2.522	2.308	0.082
Portal	2.946	2.846	0.322
Fibrosis	3.587	3.436	0.428
Portal lymphoid reaction	4.098	3.949	0.363
Damage of bile duct	0.380	0.256	0.216
Portal sclerotic change	0.076	0.077	0.990
Perivenular fibrosis	1.133	1.000	0.447
Pericellular fibrosis	1.163	0.821	0.045
Bridging fibrosis	0.957	0.641	0.106
Irregular regeneration	2.207	1.795	0.105
Anisocytosis	1.891	1.385	0.024
Bulging	0.326	0.436	0.485
Map-like distribution	1.370	1.333	0.881
Oncocytes	1.326	1.051	0.227
Nodularity	1.185	1.231	0.849
Atypical hepatocytes	0.467	0.692	0.304
Steatosis	1.707	1.692	0.951

NOTE: Data shown as mean.

had higher expression of hepatic ISGs, whereas patients with the TT genotype showed lower expression of hepatic ISGs in CHC tissues and noncancerous background liver tissue, confirming our previous data (Fig. 2A and Supplementary Table S2). Expression of hepatic ISGs in HCC tissues was lower than in background liver tissues, with no relationship to the *IL-28B* genotype. Hierarchical clustering of 51 representative immune response-related genes from the Gene Ontology gene set of the Molecular Signatures Database indicated that their expression was upregulated in TT genotype compared with TG/GG genotype tissues, with the exception of HCC tissues (Fig. 2B and Supplementary Table S2). Upregulation of immune response-related genes suggests that hepatic inflammation is more severe in TT genotype patients, which is consistent with our histologic findings and recent studies that reported an association between high serum ALT levels and the *IL-28B* TT genotype (14, 29).

Gene expression profile of HCC tissues from *IL-28B* TT and TG/GG genotypes

We applied PAGE to identify gene sets differentially regulated between the different *IL-28B* genotypes from the whole gene expression profiles derived from HCC tissues. Analysis of groups of genes involved in a specific function enables significant differences to represent a biologically meaningful result (23). Many gene sets associated with the immune system (e.g., the immune system process, T-cell activation, regulation of T-cell activation, and T-cell proliferation) showed a significant increase in their expression in patients with HCC with the *IL-28B* TG/GG genotype (Sup-

plementary Table S3). This PAGE profile was consistent with the hierarchical clustering of 51 immune response-related genes (Fig. 2B) and suggests that the immune response to tumors might be more intensive in *IL-28B* TG/GG genotype HCC than *IL-28B* TT genotype HCC.

Lymphocyte infiltration into HCC tissues with the *IL-28B* TG/GG genotype

To verify our PAGE profile, we histologically compared HCC tissue of 20 cases of the *IL-28B* TT genotype and 12 cases of the TG/GG genotype using immunohistochemical staining with antibodies against helper T cells (CD4) and cytotoxic T cells (CD8). The mean score of the degree of CD8⁺ lymphocyte infiltration in the tumor tissue was significantly higher in the TG/GG genotype (1.75) than the TT genotype (1.175; $P = 0.047$; Supplementary Table S4). A representative case is shown in Fig. 3. There was no morphologic alteration associated with the *IL-28B* genotype. Immunohistochemical analysis showed intratumoral infiltration of CD4⁺ and CD8⁺ lymphoid cells and slight infiltration of monocytes/macrophages in HCC of the *IL-28B* TG/GG genotype, compared with little infiltration of lymphocytes or monocytes/macrophages in HCC of the *IL-28B* TT genotype.

Furthermore, the gene set differentially expressed in HCC-infiltrating mononuclear inflammatory cells from our previous study (24) was upregulated in HCC of the *IL-28B* TG/GG genotype (Z score, -9.879 ; $P < 0.001$). One-way hierarchical clustering was carried out of 122 genes involved in the gene set differentially expressed in HCC-infiltrating

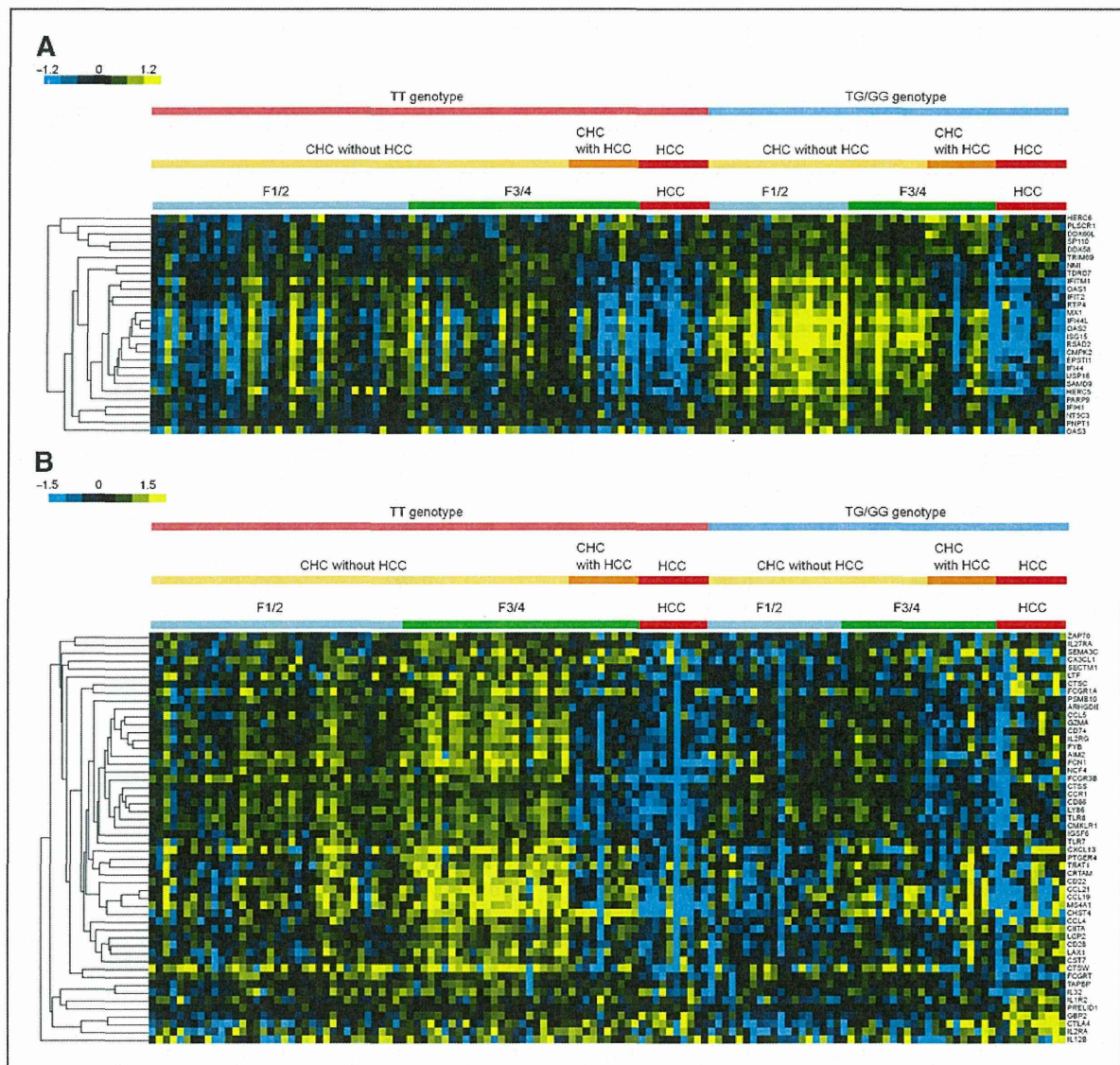


Figure 2. A, one-way hierarchical clustering of 28 representative ISGs of 111 patients with the *IL-28B* genotype. B, one-way hierarchical clustering analysis of 51 representative immune response-related genes of 111 patients with the *IL-28B* genotype.

mononuclear inflammatory cells. Most of the 122 genes were expressed at high levels in many HCC tissues of *IL-28B* TG/GG genotype patients (Supplementary Fig. S2).

Discussion

IL-28B is a recently identified, novel IFN- λ family member that shares the same biologic properties as type I IFNs (9). Recent reports have shown a significant association between *IL-28B* allelic variants and treatment outcome in CHC (11, 12). *IL-28B* genotyping is therefore considered to be a suitable pretreatment predictor of treatment response for individual patients, and also an indicator of biochemical and histologic findings in

patients infected with HCV (14). In this study, we determined that the *IL-28B* genotype is associated with HCC recurrence in patients with CHC as patients with the *IL-28B* TT genotype showed a significantly higher incidence of recurrence than those with the *IL-28B* TG/GG genotype after curative therapy. To our knowledge, this is the first study to reveal an association between the *IL-28B* genotype and HCC recurrence and molecular features in patients with CHC.

To date, there are several contradicting results about the association of the *IL-28B* genotype and progression of liver disease including the development of HCC. Fabris and colleagues and Eurich and colleagues reported that

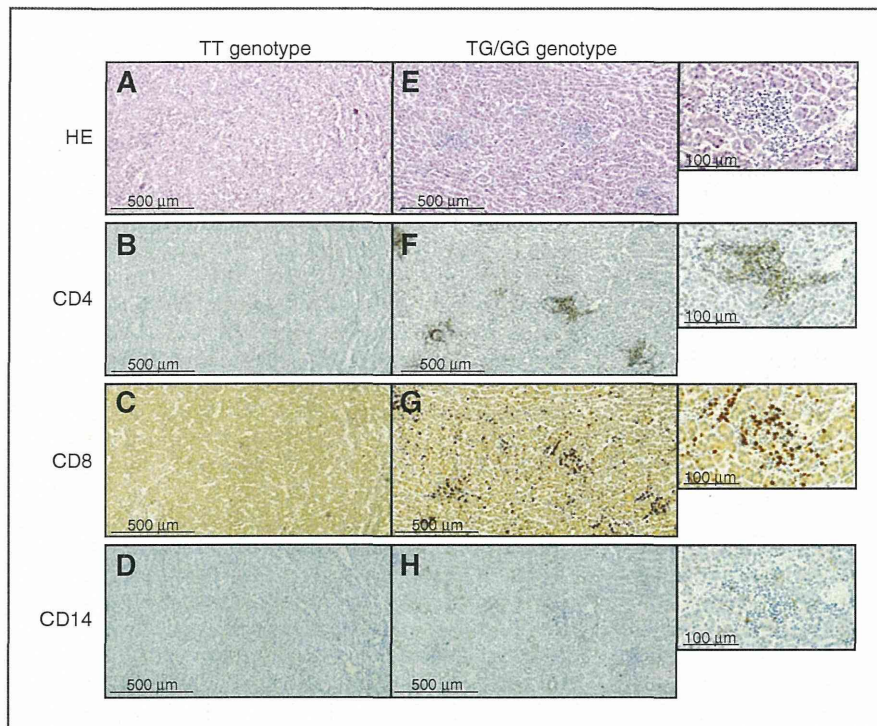


Figure 3. Expression of CD4, CD8, and CD14 in tumor-infiltrating mononuclear cells in HCC tissues. Immunohistochemical analysis of noncancerous liver tissues of *IL-28B* TT (A–D) and TG/GG genotypes (E–H). Samples were analyzed by hematoxylin and eosin staining (A and E), CD4 staining (B and F), CD8 staining (C and G), and CD14 staining (D and H).

patients with a T allele in rs12979860 (G allele in rs8099917) were at a high risk of progressing to liver cirrhosis and HCC (35, 36), however, these reports have not yet been confirmed by others. A large-scale European genome-wide association study (GWAS) recently identified a weak protective role for the rs12979860 T allele in the progression of fibrosis during HCV infection (37), whereas a Japanese GWAS identifying a susceptibility locus for HCV-induced HCC found no association of rs12979860 and rs8099917 SNPs with HCC (38). In support of these findings, Joshita and colleagues reported no association between the *IL-28B* genotype and the incidence of primary HCC (39). These results show a good concordance with those of the present study, which revealed that the *IL-28B* genotype was not associated with HCC incidence before treatment (Table 1). Furthermore, closer histologic assessment showed a high score of periportal inflammation and pericellular fibrosis in the rs8099917 TT genotype (CC in rs12979860). This suggests that our patient selection process was not biased, and that our results are in agreement with the Japanese study and are comparable with the European study.

To date, the reasons for contradicting results about the association of the *IL-28B* genotype and progression of liver disease have not been clear, however, clinical bias such as patient number, history of treatment, virus genotype, and titer and racial differences may affect the results. It should be noted that significant differences in genotype frequencies with respect to ethnic/racial groups have previously been reported for *IL-28B* SNPs (11). To overcome these limita-

tions, a future cross-sectional prospective study should be conducted.

Several risk factors for HCC recurrence have previously been reported, including the presence of cirrhosis, high AFP levels, and multiplicity of tumors (7, 8). However, multivariate analysis and the bootstrap procedure of the present study revealed that the *IL-28B* genotype was independent indicators for recurrence, suggesting that it is stronger predictors of HCC recurrence than other factors.

The expression of hepatic ISGs was higher in *IL-28B* TG/GG genotype patients than *IL-28B* TT genotype patients with CHC in this study. This confirms our previous findings in a different cohort and those of another research group (13, 40). Several ISGs have been reported to have antiproliferative and proapoptotic functions (41, 42), and IFN- α (type I IFN) has also been found to inhibit metastasis and human HCC recurrence after curative resection mediated by angiogenesis (43). Indeed, *IL-28B* rs8099917 is associated with early HCC recurrence (<1 year), possibly because of the intrahepatic metastasis of HCC in this study (Fig. 1 and Supplementary Table S5). These reports and our findings suggest that high expression of hepatic ISGs might cause the low HCC recurrence in the *IL-28B* TG/GG genotype, although the mechanism of this association remains unknown.

Microarray, histologic, and immunohistochemical analysis in the present study showed that the immune response was more severe in chronic hepatitis and noncancerous tissue of *IL-28B* TT genotype compared with TG/GG genotype patients. Serum ALT levels were also higher in the

IL-28B TT genotype, albeit not significantly. These results support previous findings that showed higher serum ALT levels and more severe liver inflammation in TT genotype compared with TG/GG genotype patients with HCC (14, 29). Irregular regeneration of hepatocytes develops as a result of repeated cycles of necrosis and regeneration of hepatocytes and was previously reported to be an important predictive factor for the development of HCC (26). We histologically showed that the degree of hepatocyte anisocytosis was more severe in noncancerous livers of TT genotype than TG/GG genotype patients, perhaps because of *IL-28B* genotype-dependent hepatic inflammation. This might also affect the late recurrence of HCC (>1 year) as a result of the multicentric occurrence of HCC in background liver disease. In the late recurrence group, *IL-28B* TT genotype patients showed a shorter TTR than *IL-28B* TG/GG genotype patients although this did not reach statistical significance ($P = 0.086$; Supplementary Fig. S3; Supplementary Table S6).

Previous studies showed that the gene expression profile of noncancerous liver tissue was associated with late recurrence HCC and the multicentric occurrence of HCC (44). However, the gene set expression of these studies did not differ between the *IL-28B* TT and TG/GG genotypes in the present study. Although the reason for this discrepancy is unclear, the *IL-28B* genotype may affect early recurrence more than late recurrence, and the limited number of patients and the short follow-up period may affect statistical comparisons. Therefore, further investigations with a large series of patients are necessary to clarify whether *IL-28B* genotype-dependent inflammation influences HCC recurrence.

On the other hand, the gene expression profile and histologic analyses showed that more lymphocytes infiltrate into the tumor tissue of the *IL-28B* TG/GG genotype than the TT genotype. Chew and colleagues previously showed that 14 intratumoral immune gene signatures were able to identify molecular cues driving the tumor infiltration of lymphocytes and predict the survival of patients with HCC, particularly during the early stages of disease (45). We can confirm that the expression of some of these 14 genes was higher in TG/GG genotype than TT genotype patients (Supplementary Fig. S4), supporting the association of the *IL-28B* genotype, HCC recurrence, and histologic findings. The presence of lymphocyte infiltration in HCC was also reported as a negative predictor of HCC recurrence after liver transplantation (46), and this phenomenon may contribute to a lower incidence of HCC recurrence in the TG/GG genotype.

It may seem contradictory that the immune response in noncancerous liver was more severe in TT genotype than TG/GG genotype patients despite the fact that the expression of immune genes was higher in tumor tissue and more lymphocytes infiltrated the tumor in the TG/GG genotype compared with the TT genotype. Although we are unable to explain this contradiction, it is conceivable that the host immune reaction has a differential role between tumor and nontumor tissue.

Moreover, HCV-specific T-cell immune responses, which are essential for disease control, are attenuated in patients with CHC, and T-cell exhaustion has recently been implicated in the deficient control of chronic viral infections. On the other hand, little is known on self- and tumor-specific T-cell responses in patients with HCC. While several reports have shown the existence of exhausted T cells in a tumor environment, impaired T-cell responses to tumors are unlikely to be simply explained by T-cell exhaustion (47).

Energy or other functional statuses such as suppressive immunity by tumor cells should be considered in tumor immunity. Therefore, differences in immunity to viral antigens and self- and tumor-antigens could explain our findings, although further work should be carried out to confirm these conclusions. We have preliminarily confirmed that the ratio of regulatory T cells is higher in the peripheral blood of *IL-28B* TT genotype HCC patients than *IL-28B* TG/GG genotype patients, although there is no significant difference between non-HCC *IL-28B* TT genotype and *IL-28B* TG/GG genotype patients (data not shown). Although the cause of this phenomenon is unclear, our gene expression profile of noncancerous liver and tumor tissues suggests paradoxical roles for the immune response in CHC and HCC depending on *IL-28B* genotype; it will be necessary to clarify these mechanisms in future investigations.

Recently, a sustained virologic response (SVR) to CHC antiviral treatment was shown to be associated with a lower risk of HCC recurrence (48). Although we did not include patients with SVR in the current study, we nevertheless observed that they showed a longer recurrence-free survival than patients infected with HCV, independent of *IL-28B* genotype (data not shown). This result together with the association between the *IL-28B* genotype and response to antiviral treatment promotes recommendations for aggressive CHC antiviral treatment, especially in cases with the *IL-28B* TT genotype.

RFA is a recently developed technique and its efficacy has been reported equal to that of surgical resection, especially in early-stage HCC (3–6). In the European Association for the Study of the Liver–European Organisation for Research and Treatment of Cancer (EASL-EORTC) guidelines, RFA is considered the standard care for patients with Barcelona Clinic Liver Cancer stage 0-A tumors not suitable for surgery and whether or not RFA can be considered a competitive alternative to resection is uncertain (49). In our study, the local tumor progression rate was not statistically different between RFA and resection cases. However, further studies with an appropriate sample population are necessary to clarify the comparison of RFA and resection. The present study has some limitations. It was a retrospective cohort and a single-center study, so it was difficult to completely eliminate bias. Further prospective studies of a larger series of patients should be conducted to validate our results. As a consequence of the small sample size and even smaller number of patients undergoing surgical resection, we could not show an association between *IL-28B* genotype and HCC

recurrence in the surgical resection group (data not shown). However, we did find no significant difference in TTR between REA and surgical resection, confirming previous findings.

In conclusion, we found that the *IL-28B* rs8099917 TT genotype is associated with shorter TTR in patients with HCC with CHC. Microarray analysis showed a high expression of ISGs in background liver and high expression of immune system-related genes in tumor tissues of the *IL-28B* TG/GG genotype. Histologic findings also showed that more lymphocytes infiltrated into tumor tissues in the TG/GG genotype. The *IL-28B* genotype therefore is a candidate useful genetic marker to predict HCC recurrence as well as the response to pegylated-IFN and ribavirin combination therapy for CHC.

Disclosure of Potential Conflicts of Interest

No potential conflicts of interest were disclosed.

References

1. Yang JD, Roberts LR. Hepatocellular carcinoma: a global view. *Nat Rev Gastroenterol Hepatol* 2010;7:448–58.
2. Cha C, DeMatteo RP, Blumgart LH. Surgery and ablative therapy for hepatocellular carcinoma. *J Clin Gastroenterol* 2002;35(5 Suppl 2): S130–7.
3. Lü M, Kuang M, Liang L, Xie X, Peng B, Liu G, et al. Surgical resection versus percutaneous thermal ablation for early-stage hepatocellular carcinoma: a randomized clinical trial. *Zhonghua Yi Xue Za Zhi* 2006; 86:801–5.
4. Chen M-S, Li J-Q, Zheng Y, Guo R-P, Liang H-H, Zhang Y-Q, et al. A prospective randomized trial comparing percutaneous local ablative therapy and partial hepatectomy for small hepatocellular carcinoma. *Ann Surg* 2006;243:321–8.
5. Hong SN, Lee S-Y, Choi MS, Lee JH, Koh KC, Paik SW, et al. Comparing the outcomes of radiofrequency ablation and surgery in patients with a single small hepatocellular carcinoma and well-preserved hepatic function. *J Clin Gastroenterol* 2005;39: 247–52.
6. Nishikawa H, Inuzuka T, Takeda H, Nakajima J, Matsuda F, Sakamoto A, et al. Comparison of percutaneous radiofrequency thermal ablation and surgical resection for small hepatocellular carcinoma. *BMC Gastroenterol* 2011;11:143.
7. Koike Y, Shiratori Y, Sato S, Obi S, Teratani T, Imamura M, et al. Risk factors for recurring hepatocellular carcinoma differ according to infected hepatitis virus—an analysis of 236 consecutive patients with a single lesion. *Hepatology* 2000;32:1216–23.
8. Yamanaka Y, Shiraki K, Miyashita K, Inoue T, Kawakita T, Yamaguchi Y, et al. Risk factors for the recurrence of hepatocellular carcinoma after radiofrequency ablation of hepatocellular carcinoma in patients with hepatitis C. *World J Gastroenterol* 2005;11:2174–8.
9. Sheppard P, Kindsvogel W, Xu W, Henderson K, Schlutsmeyer S, Whitmore TE, et al. IL-28, IL-29 and their class II cytokine receptor IL-28R. *Nat Immunol* 2003;4:63–8.
10. Li M, Liu X, Zhou Y, Su SB. Interferon-lambdas: the modulators of antiviral, antitumor, and immune responses. *J Leukoc Biol* 2009; 86:23–32.
11. Ge D, Fellay J, Thompson AJ, Simon JS, Shianna KV, Urban TJ, et al. Genetic variation in IL28B predicts hepatitis C treatment-induced viral clearance. *Nature* 2009;461:399–401.
12. Tanaka Y, Nishida N, Sugiyama M, Kurosaki M, Matsuura K, Sakamoto N, et al. Genome-wide association of IL28B with response to pegylated interferon-alpha and ribavirin therapy for chronic hepatitis C. *Nat Genet* 2009;41:1105–9.
13. Honda M, Sakai A, Yamashita T, Nakamoto Y, Mizukoshi E, Sakai Y, et al. Hepatic ISG expression is associated with genetic variation in interleukin 28B and the outcome of IFN therapy for chronic hepatitis C. *Gastroenterology* 2010;139:499–509.
14. Abe H, Ochi H, Maekawa T, Hayes CN, Tsuge M, Miki D, et al. Common variation of IL28 affects gamma-GTP levels and inflammation of the liver in chronically infected hepatitis C virus patients. *J Hepatol* 2010;53:439–43.
15. Rauch A, Kutalik Z, Descombes P, Cai T, Di Iulio J, Mueller T, et al. Genetic variation in IL28B is associated with chronic hepatitis C and treatment failure: a genome-wide association study. *Gastroenterology* 2010;138:1338–45, 1345.e1–7.
16. Kudo M, Okanoue T. Management of hepatocellular carcinoma in Japan: consensus-based clinical practice manual proposed by the Japan Society of Hepatology. *Oncology* 2007;72(Suppl 1):2–15.
17. Kokudo N, Makuuchi M. Evidence-based clinical practice guidelines for hepatocellular carcinoma in Japan: the J-HCC guidelines. *J Gastroenterol* 2009;44(Suppl 1):119–21.
18. Matsui O. Imaging of multistep human hepatocarcinogenesis by CT during intra-arterial contrast injection. *Intervirology* 2004;47:271–6.
19. Liver Cancer Study Group of Japan. The general rules for the clinical and pathological study of primary liver cancer. 5th ed. Tokyo, Japan: Kanahara Shuppan; 2009.
20. R Development Core Team. R: a language and environment for statistical computing. Vienna, Austria: R Foundation for Statistical Computing; 2012. [cited 2012 May 1]. Available from: <http://www.r-project.org/>.
21. Gentleman RC, Carey VJ, Bates DM, Bolstad B, Dettling M, Dudoit S, et al. Bioconductor: open software development for computational biology and bioinformatics. *Genome Biol* 2004;5:R80.
22. Subramanian A, Tamayo P, Mootha VK, Mukherjee S, Ebert BL, Gillette MA, et al. Gene set enrichment analysis: a knowledge-based approach for interpreting genome-wide expression profiles. *Proc Natl Acad Sci U S A* 2005;102:15545–50.
23. Kim S-Y, Volsky DJ. PAGE: parametric analysis of gene set enrichment. *BMC Bioinformatics*. 2005;6:144.
24. Sakai Y, Honda M, Fujinaga H, Tatsumi I, Mizukoshi E, Nakamoto Y, et al. Common transcriptional signature of tumor-infiltrating mononuclear inflammatory cells and peripheral blood mononuclear cells in hepatocellular carcinoma patients. *Cancer Res* 2008;68:10267.
25. Desmet VJ, Gerber M, Hoofnagle JH, Manns M, Scheuer PJ. Classification of chronic hepatitis: diagnosis, grading and staging. *Hepatology* 1994;19:1513–20.

Authors' Contributions

Conception and design: M. Honda, Y. Sakai, M. Moriyama, S. Kaneko

Development of methodology: M. Moriyama

Acquisition of data (provided animals, acquired and managed patients, provided facilities, etc.): Y. Hodo, A. Tanaka, K. Arai, T. Yamashita, T. Yamashita, A. Sakai, Y. Nakanuma, M. Moriyama, S. Kaneko

Analysis and interpretation of data (e.g., statistical analysis, biostatistics, computational analysis): Y. Hodo, M. Honda, M. Sasaki, M. Moriyama

Writing, review, and/or revision of the manuscript: Y. Hodo, M. Honda, M. Moriyama

Administrative, technical, or material support (i.e., reporting or organizing data, constructing databases): Y. Hodo, A. Tanaka, Y. Nomura, K. Arai, E. Mizukoshi, M. Sasaki, M. Moriyama, S. Kaneko

Study supervision: Y. Sakai, E. Mizukoshi, M. Moriyama

The costs of publication of this article were defrayed in part by the payment of page charges. This article must therefore be hereby marked *advertisement* in accordance with 18 U.S.C. Section 1734 solely to indicate this fact.

Received May 25, 2012; revised December 20, 2012; accepted February 7, 2013; published OnlineFirst February 20, 2013.

26. Ueno Y, Moriyama M, Uchida T, Arakawa Y. Irregular regeneration of hepatocytes is an important factor in the hepatocarcinogenesis of liver disease. *Hepatology* 2001;33:357–62.
27. Sauerbrei W, Schumacher M. A bootstrap resampling procedure for model building: application to the Cox regression model. *Stat Med* 1992;11:2093–109.
28. Harrell FE Jr. rms: regression modeling strategies. 2012. [cited 2012 May 1]. Available from: <http://cran.r-project.org/package=rms>.
29. Akuta N, Suzuki F, Hirakawa M, Kawamura Y, Yatsuji H, Sezaki H, et al. Amino acid substitution in hepatitis C virus core region and genetic variation near the interleukin 28B gene predict viral response to telaprevir with peginterferon and ribavirin. *Hepatology* 2010;52:421–9.
30. Miyamura T, Kanda T, Nakamoto S, Wu S, Fujiwara K, Imazeki F, et al. Hepatic STAT1-nuclear translocation and interleukin 28B polymorphisms predict treatment outcomes in hepatitis C virus genotype 1-infected patients. *PLoS ONE* 2011;6:e28617.
31. Ochi H, Maekawa T, Abe H, Hayashida Y, Nakano R, Imamura M, et al. IL-28B predicts response to chronic hepatitis C therapy—fine-mapping and replication study in Asian populations. *J Gen Virol* 2011;92:1071–81.
32. Database of single nucleotide polymorphisms (dbSNP). Bethesda, MD: National Center for Biotechnology Information, National Library of Medicine. dbSNP accession:rs8099917 (dbSNP Build ID: 137). [cited 2012 Oct 1]. Available from: <http://www.ncbi.nlm.nih.gov/SNP/>.
33. Shiina S, Tateishi R, Arano T, Uchino K, Enooku K, Nakagawa H, et al. Radiofrequency ablation for hepatocellular carcinoma: 10-year outcome and prognostic factors. *Am J Gastroenterol* 2012;107:569–77.
34. Lencioni R, Cioni D, Crocetti L, Franchini C, Pina C Della, Lera J, et al. Early-stage hepatocellular carcinoma in patients with cirrhosis: long-term results of percutaneous image-guided radiofrequency ablation. *Radiology* 2005;234:961–7.
35. Fabris C, Falletti E, Cusigh A, Bitetto D, Fontanini E, Bignulin S, et al. IL-28B rs12979860 C/T allele distribution in patients with liver cirrhosis: role in the course of chronic viral hepatitis and the development of HCC. *J Hepatol* 2011;54:716–22.
36. Eurich D, Boas-Knoop S, Bahra M, Neuhaus R, Somasundaram R, Neuhaus P, et al. Role of IL28B polymorphism in the development of hepatitis C virus-induced hepatocellular carcinoma, graft fibrosis, and posttransplant antiviral therapy. *Transplantation* 2012;93:644–9.
37. Patin E, Kutalik Z, Guergnon J, Bibert S, Nalpas B, Jouanguy E, et al. Genome-wide association study identifies variants associated with progression of liver fibrosis from HCV infection. *Gastroenterology* 2012;143:1244–52.e12.
38. Kumar V, Kato N, Urabe Y, Takahashi A, Muroyama R, Hosono N, et al. Genome-wide association study identifies a susceptibility locus for HCV-induced hepatocellular carcinoma. *Nat Genet* 2011;43:455–8.
39. Joshita S, Umemura T, Katsuyama Y, Ichikawa Y, Kimura T, Morita S, et al. Association of IL28B gene polymorphism with development of hepatocellular carcinoma in Japanese patients with chronic hepatitis C virus infection. *Hum Immunol* 2012;73:298–300.
40. Urban TJ, Thompson AJ, Bradrick SS, Fellay J, Schuppan D, Cronin KD, et al. IL28B genotype is associated with differential expression of intrahepatic interferon-stimulated genes in patients with chronic hepatitis C. *Hepatology* 2010;52:1888–96.
41. Besch R, Poeck H, Hohenauer T, Senft D, Häcker G, Berking C, et al. Proapoptotic signaling induced by RIG-I and MDA-5 results in type I interferon-independent apoptosis in human melanoma cells. *J Clin Invest* 2009;119:2399–411.
42. Stawowczyk M, Van Scoy S, Kumar KP, Reich NC. The interferon stimulated gene 54 promotes apoptosis. *J Biol Chem* 2011;286:7257–66.
43. Wang L, Wu W-Z, Sun H-C, Wu X-F, Qin L-X, Liu Y-K, et al. Mechanism of interferon alpha on inhibition of metastasis and angiogenesis of hepatocellular carcinoma after curative resection in nude mice. *J Gastrointest Surg* 2003;7:587–94.
44. Hoshida Y, Villanueva A, Kobayashi M, Peix J, Chiang DY, Camargo A, et al. Gene expression in fixed tissues and outcome in hepatocellular carcinoma. *N Engl J Med* 2008;359:1995–2004.
45. Chew V, Chen J, Lee D, Loh E, Lee J, Lim KH, et al. Chemokine-driven lymphocyte infiltration: an early intratumoural event determining long-term survival in resectable hepatocellular carcinoma. *Gut* 2012;61:427–38.
46. Unitt E, Marshall A, Gelson W, Rushbrook SM, Davies S, Vowler SL, et al. Tumour lymphocytic infiltrate and recurrence of hepatocellular carcinoma following liver transplantation. *J Hepatol* 2006;45:246–53.
47. Baitsch L, Baumgaertner P, Devèvre E, Raghav SK, Legat A, Barba L, et al. Exhaustion of tumor-specific CD8⁺ T cells in metastases from melanoma patients. *J Clin Invest* 2011;121:2350–60.
48. Miyatake H, Kobayashi Y, Iwasaki Y, Nakamura S-I, Ohnishi H, Kuwaki K, et al. Effect of previous interferon treatment on outcome after curative treatment for hepatitis C virus-related hepatocellular carcinoma. *Dig Dis Sci* 2012;57:1092–101.
49. European Association For The Study Of The Liver; European Organisation For Research And Treatment Of Cancer. EASL-EORTC clinical practice guidelines: management of hepatocellular carcinoma. *J Hepatol* 2012;56:908–43.

**Title: Gd-EOB-DTPA-enhanced Magnetic Resonance Imaging and Alpha-fetoprotein
Predict Prognosis of Early-Stage Hepatocellular Carcinoma**

Authors: Taro Yamashita^{1,2}, Azusa Kitao³, Osamu Matsui³, Takehiro Hayashi², Kouki Nio², Mitsumasa Kondo², Naoki Ohno⁴, Toshiaki Miyati⁴, Hikari Okada², Tatsuya Yamashita², Eishiro Mizukoshi², Masao Honda², Yasuni Nakanuma⁵, Hiroyuki Takamura⁶, Tetsuo Ohta⁶, Yasunari Nakamoto⁷, Masakazu Yamamoto⁸, Tadatoshi Takayama⁹, Shigeki Arii¹⁰, Xin Wei Wang¹¹, and Shuichi Kaneko²

Keywords: Hepatocellular Carcinoma Subtype, Organic Anion Transporting Polypeptides, Hepatocyte Nuclear Factor 4 Alpha, Forkhead Box M1, Stem/Maturational Status

Affiliations:

¹Department of General Medicine, Kanazawa University Graduate School of Medical Science, Kanazawa, Ishikawa, Japan.

²Department of Gastroenterology, Kanazawa University Graduate School of Medical Science, Kanazawa, Ishikawa, Japan.

³Department of Radiology, Kanazawa University Graduate School of Medical Science, Kanazawa, Ishikawa, Japan.

⁴Faculty of Health Sciences, Institute of Medical, Pharmaceutical and Health Sciences, Kanazawa University, Kanazawa, Ishikawa, Japan.

This article has been accepted for publication and undergone full peer review but has not been through the copyediting, typesetting, pagination and proofreading process which may lead to differences between this version and the Version of Record. Please cite this article as doi: 10.1002/hep.27093

⁵Department of Pathology, Kanazawa University Graduate School of Medical Science, Kanazawa, Ishikawa, Japan.

⁶Department of Gastroenterologic Surgery, Kanazawa University Graduate School of Medical Science, Kanazawa, Ishikawa, Japan.

⁷Second Department of Internal Medicine, Fukui University School of Medicine, Fukui, Japan.

⁸Department of Surgery, Institute of Gastroenterology, Tokyo Women's Medical University, Tokyo, Japan.

⁹Department of Digestive Surgery, Nihon University School of Medicine, Tokyo, Japan.

¹⁰Department of Hepato-Biliary-Pancreatic Surgery, Tokyo Medical and Dental University, Tokyo, Japan.

¹¹Laboratory of Human Carcinogenesis, Center for Cancer Research, National Cancer Institute, Bethesda, Maryland, USA

Contact: Taro Yamashita M.D., Ph.D.

Assistant Professor, Department of Gastroenterology/General Medicine, Kanazawa University Graduate School of Medical Science, 13-1 Takara-Machi, Kanazawa, Ishikawa 920-8641, Japan

TEL.: +81-76-265-2235

FAX: +81-76-234-4250

E-mail: taroy@m-kanazawa.jp

Abbreviations: AFP, alpha-fetoprotein; BCLC, Barcelona Clinic Liver Cancer; EOB-MRI, gadolinium ethoxybenzyl diethylenetriamine pentaacetic acid-enhanced magnetic resonance imaging; FOXM1, forkhead box protein M1; Gd-EOB-DTPA, gadolinium ethoxybenzyl diethylenetriamine pentaacetic acid; HCC, hepatocellular carcinoma; HNF4 α , hepatocyte nuclear factor 4 alpha; IHC, immunohistochemistry; MRI, magnetic resonance imaging; NOD/SCID, nonobese diabetic, severe combined immunodeficient; OATPs, organic anion transporting polypeptides; qRT-PCR, quantitative reverse-transcription polymerase chain reaction; SI, signal intensity; TNM, tumor node metastasis.

Grant Support:

This study was supported by Health and Labor Sciences Research Grants for “Development of novel molecular markers and imaging modalities for earlier diagnosis of hepatocellular carcinoma,” Grants from the Ministry of Education, Culture, Sports, Science, and Technology of Japan, the National Cancer Center Research and Development Fund (23-B-5), and the Intramural Research Program Grant (Z01 BC 010313) of the Center for Cancer Research, US National Cancer Institute.

Abstract

The survival of patients with hepatocellular carcinoma (HCC) is often individually different even after surgery for early-stage tumors. Gadolinium ethoxybenzyl diethylenetriamine pentaacetic acid (Gd-EOB-DTPA)-enhanced magnetic resonance imaging (MRI) has been introduced recently to evaluate hepatic lesions with regard to vascularity and the activity of the organic anion transporter OATP1B3. Here, we report that Gd-EOB-DTPA-enhanced MRI (EOB-MRI) in combination with serum alpha-fetoprotein (AFP) status reflects the stem/maturation status of HCC with distinct biology and prognostic information. Gd-EOB-DTPA uptake in the hepatobiliary phase was observed in approximately 15% of HCCs. This uptake correlated with low serum AFP levels, maintenance of hepatocyte function with the up-regulation of *OATP1B3* and *HNF4A* expression, and good prognosis. By contrast, HCC showing reduced Gd-EOB-DTPA uptake with high serum AFP levels was associated with poor prognosis and the activation of the oncogene *FOXMI*. Knockdown of *HNF4A* in HCC cells showing Gd-EOB-DTPA uptake resulted in the increased expression of *AFP* and *FOXMI* and the loss of *OATP1B3* expression accompanied by morphological changes, enhanced tumorigenesis, and loss of Gd-EOB-DTPA uptake *in vivo*. HCC classification based on EOB-MRI and serum AFP levels predicted overall survival in a single-institution cohort (n = 70), and its prognostic utility was validated independently in a multi-institution cohort of early-stage HCCs (n = 109). *Conclusion:* This non-invasive classification system is molecularly based on the stem/maturation status of HCCs and can be incorporated into current staging practices to improve management algorithms, especially in the early stage of disease.

Liver cancer is the fifth most commonly diagnosed cancer and the second most frequent cause of cancer death in men worldwide (1). Among primary liver cancers, hepatocellular carcinoma (HCC) represents the major histological subtype, accounting for 70–86% of cases of primary liver cancer (1). Several staging systems are currently available for HCC classification and include tumor node metastasis (TNM) and Barcelona Clinic Liver Cancer (BCLC) staging, which are based on tumor number and size, vascular invasion, metastatic status, hepatic reserve, and performance status (2). These systems can provide an approximate estimate of patients' survival, but patients diagnosed at the same disease stage sometimes show a different prognosis. This is most likely because these systems do not include an assessment of the malignant phenotype of the tumor, which would be especially important in those patients diagnosed at the early stage of disease. To overcome these limitations, gene expression profiling technologies have been applied to classify HCC. In particular, the stemness of HCC is currently of great interest because its gene expression profile reflects the malignant nature of the tumor (3–7). However, the application of these new technologies still needs to be validated externally prior to their implementation in clinical practice.

The hallmark of HCC diagnosis has been image analysis based on vascularity. Gadolinium ethoxybenzyl diethylenetriamine pentaacetic acid (Gd-EOB-DTPA) is a liver-specific magnetic resonance imaging (MRI) contrast agent introduced specifically to improve the detection of liver lesions (8). Gd-EOB-DTPA-enhanced MRI (EOB-MRI) has been used to evaluate liver tumors in Europe since 2004, in the USA and Japan since 2008, and in China since 2010. Gd-EOB-DTPA is characterized by its rapid and specific uptake by hepatocytes via organic anion transporting polypeptides (OATPs) expressed in the sinusoidal membrane. Therefore, Gd-EOB-DTPA uptake in the liver is considered to reflect hepatocyte function (9).

Among OATP1A2, 1B1, 1B3, and 2B1, only OATP1B3 expression was found to correlate with the enhancement ratio on EOB-MRI, indicating that it transports Gd-EOB-DTPA into HCC cells (10). It is generally accepted that approximately 85% of HCCs show hypo-intensity in the hepatobiliary phase of EOB-MRI compared to the non-cancerous background liver, with a reduction of OATP1B3 protein or *OATP1B3* gene expression in the tumor (10, 11). However, atypical Gd-EOB-DTPA uptake in the hepatobiliary phase is observed in the remaining 15% of HCCs, and the molecular phenotype and clinical features of these HCCs remain to be elucidated.

We hypothesized that EOB-MRI findings may vary in different tumor subtypes with distinct biology. Therefore, in this study, we evaluated the molecular profiles of HCCs in a single institute cohort determined from the EOB-MRI findings using quantitative reverse-transcription polymerase chain reaction (qRT-PCR), microarray, and immunohistochemistry (IHC) analyses. To clarify the clinical utility of the EOB-MRI findings, we also evaluated the prognosis of a multicenter cohort of patients with early-stage HCC who underwent radical resection.

Materials and Methods

Patients. A total of 417 patients who received surgical resection for HCC were enrolled in this study. Seventy patients underwent EOB-MRI for the diagnosis of HCC and received surgical resection at Kanazawa University Hospital from 2008 to 2011. Survival analysis was performed in this single-institute cohort (Cohort 1), and prognosis was evaluated every 6 months. The final evaluation of survival was performed in October 2011. From these 70 patients, 62 tumor and non-tumor samples were snap-frozen in liquid nitrogen and used for qRT-PCR.

For microarray analysis, we assessed 238 patients who received surgical resection of HCC at the Liver Cancer Institute of Fudan University. EOB-MRI was not performed in these patients because Gd-EOB-DTPA had not yet been introduced in China. Their clinicopathologic characteristics and prognostic data have been described previously (12).

To evaluate the survival of early-stage HCCs, we enrolled 109 patients who received EOB-MRI and surgical resection at Tokyo Medical and Dental University Hospital, Tokyo Women's Medical University Hospital, Nihon University School of Medicine Itabashi Hospital, Niigata University Medical & Dental Hospital, Hyogo College of Medicine Hospital, or Kurume University Hospital from 2008 to 2009 (Cohort 2). The prognosis of these patients was evaluated every year, and the final evaluation of survival was performed in February 2012.

This study was approved by the institutional review board at each study center, and all patients provided written informed consent.

EOB-MRI. EOB-MRI was performed before surgical resection using a 1.5 or 3.0 Tesla MRI system with a fat-suppressed 2D or 3D gradient echo T1-weighted sequence (TR/TE = 3.2–3.6/1.6–2.3 ms, flip angle 10–15°, field of view 33–42 cm, matrix 128–192 × 256–512, slice thickness 4.0–8.0 mm). A dose of 0.025 mmol/kg Gd-EOB-DTPA (Primovist; Bayer Schering

Pharma, Berlin, Germany) was injected intravenously, and the hepatobiliary phase was obtained at 15–20 min after the injection.

All abdominal MRI data of the HCC patients were generated at Kanazawa University Hospital, and image analysis was performed retrospectively by two radiologists (A.K. and O.M.) without knowledge of the clinical and pathological results. The signal intensity (SI) of the tumor was measured within the region of interest, which was determined as the maximum oval area at the largest section of the tumor. The SI of the adjacent background liver was also measured within a region of interest of the same size, while avoiding large vessels. The nodules were classified into the two following types: hypo-intense HCC, which was defined as showing a lower SI than that of the surrounding liver (tumor SI/background SI < 1.0) in the hepatobiliary phase; and hyper-intense HCC, which was defined as showing an equal or higher SI (tumor SI/background SI \geq 1.0).

For the mouse study, EOB-MRI was performed using a 0.4 Tesla MRI system with a fat-suppressed 3D gradient echo T1-weighted sequence (TR/TE=66.5/4.0 ms, flip angle 40°, field of view 10 cm, matrix 224 × 192, slice thickness 1.0 mm). A dose of 0.025 mmol/kg Gd-EOB-DTPA (Bayer Schering Pharma) was injected through the tail vein, and the hepatobiliary phase was obtained at 12–20 min after the injection.

Xenotransplantation of primary HCC in immunodeficient mice and *HNF4A* knockdown.

Primary HCC tissue was dissected and digested in 1 mg/mL type 4 collagenase solution (Sigma-Aldrich Japan, Tokyo, Japan) at 37°C for 15–30 min. Contaminated red blood cells were lysed with an ammonium chloride solution (STEMCELL Technologies, Vancouver, BC, Canada) on ice for 5 min. CD45⁺ leukocytes and annexin V⁺ apoptotic cells were removed by an autoMACS-pro cell separator and magnetic beads (Miltenyi Biotec K.K., Tokyo, Japan). The cells were

suspended 1:1 in 200 μ L Dulbecco's modified Eagle's medium and Matrigel (BD Biosciences) and injected subcutaneously into 6-week-old NOD/SCID mice (NOD/NCrCRI-*Prkdc*^{scid}) purchased from Charles River Laboratories, Inc. (Wilmington, MA). EOB-MRI was performed to evaluate Gd-EOB-DTPA uptake in the subcutaneous tumor at the hepatobiliary phase, and the subcutaneous tumor was dissected and digested as described above, and subsequently cultured in Dulbecco's modified Eagle's medium. *HNF4A* knockdown was performed using pGFP-V-RS vectors (OriGene Technologies, Inc., Rockville, MD), allowing stable delivery of the shRNA expression cassette against *HNF4A* or scramble sequence into host cells via a replication-deficient retrovirus. Infected HCC cells were grown in Dulbecco's modified Eagle's medium containing 1 μ g/mL puromycin (Sigma-Aldrich Japan) for 7 days to establish stable shRNA-expressing HCC cells. Western blotting and immunofluorescence analyses were performed using an anti-human HNF4 α C11F12 antibody (Cell Signaling Technology, Danvers, MA) and a mouse monoclonal anti-human OATP1B3 MDQ/5F260 antibody (Novus Biologicals, Littleton, CO), essentially as described previously (13). Control or Sh-HNF4A-transfected HCC cells were injected subcutaneously into NOD/SCID mice, and tumor volume and survival were evaluated every 2–3 days. The protocol was approved by the Kanazawa University Animal Care and Use Committee and the Kanazawa University Genetic Modification Experiment Committee.

Microarray analysis. The 238 HCC cases from the Liver Cancer Institute of Fudan University with available microarray data and clinicopathologic and prognostic data have been described previously (12). BRB-ArrayTools software (version 3.8.1) was used for class comparison analysis. Hierarchical clustering analysis was performed with GENESIS software (version 1.6.0 beta). Canonical pathway and transcription factor analyses were performed using MetaCore

software (<http://www.genego.com>). Interaction network analysis was performed using Ingenuity Pathway Analysis software (<http://www.ingenuity.com>).

qRT-PCR analysis. Total RNA was extracted using an RNeasy Mini Kit (QIAGEN, Valencia, CA) according to the manufacturer's instructions. The expression of selected genes was determined in triplicate using the Applied Biosystems 7900HT Sequence Detection System (Applied Biosystems, Foster City, CA) and the $-\Delta\Delta CT$ method. The following probes were used: *AFP*, Hs00173490_m1; *FOXMI*, Hs01073586_m1; *OATP1B3*, Hs00251986_m1; *CYP3A4*, Hs00430021_m1; and *18S*, Hs99999901_s1 (Applied Biosystems).

IHC analysis. IHC was performed using Envision+ kits (DAKO Japan, Tokyo, Japan) as described previously (14). Mouse monoclonal anti-human Ki-67 antigen MIB-1 (DAKO Japan), mouse monoclonal anti-human OATP1B3 MDQ/5F260 (Novus Biologicals), rabbit monoclonal anti-human HNF4 α C11F12 (Cell Signaling Technology), mouse monoclonal anti-human FOXM1 0.T.181 (Abcam Inc., Cambridge, MA), mouse monoclonal anti-human glypican-3 1G12 (BioMosaics Inc., Burlington, VT), and mouse monoclonal anti-glutamine synthetase clone GS-6 (Millipore, Billerica, MA) antibodies were used. The staining area and intensities were evaluated in each sample and graded from 0–3 (0, 0–5%; 1, 5–25%; 2, 25–50%; 3, >50%) and 0–2 (0, negative; 1, weak; 2, strong), respectively. The sum of the area and intensity scores of each marker (IHC score) were calculated. Samples were defined as marker-high (IHC score ≥ 3) or -low (IHC score ≤ 2). The Ki-67 labeling index was calculated as described previously (14).

Statistical analysis. Mann-Whitney, χ^2 , Fisher's exact, and Kruskal-Wallis tests were used to compare the clinicopathologic characteristics and gene expression data. The correlation of the gene expression data was evaluated by Spearman's rank correlation coefficient. Kaplan-Meier

survival analysis with the log-rank test was performed to compare patient survival. All analyses were performed using GraphPad Prism software 5.0.1 (GraphPad Software, San Diego, CA).

Results

EOB-MRI findings and molecular characteristics of HCC

Nine of the 70 HCC cases (12.9%) in Cohort 1 were diagnosed with hyper-intense HCC on EOB-MRI (Figure 1A). Analysis of the clinicopathologic characteristics of hyper- or hypo-intense HCCs revealed that hyper-intense HCCs were significantly associated with low serum alpha-fetoprotein (AFP) levels (Table 1). There was no significant difference between hyper- and hypo-intense HCCs in terms of other factors, including tumor size, number, TNM and BCLC stages, surgical procedures, and elapsed time between MRI and surgery. We confirmed the overexpression of *OATP1B3*, a transporter responsible for the uptake of Gd-EOB-DTPA in hepatocytes, in hyper-intense HCCs by qRT-PCR and IHC (Figure 1B).

To understand the transcriptomic characteristics of HCCs overexpressing *OATP1B3*, we analyzed the microarray data of an additional 238 HCC cases (12). *OATP1B3*-high and -low HCCs were defined as HCCs with a T/N ratio ≥ 1.0 and < 1.0 , respectively, as used for the evaluation of hyper-intense HCCs (tumor SI/background SI ≥ 1.0). The frequency of *OATP1B3*-high HCCs was 15.1% (36 of the 238 HCC cases), almost comparable to the frequency of hyper-intense HCCs reported thus far. Class-comparison analysis yielded a total of 974 genes that were differentially expressed between *OATP1B3*-high and -low HCCs ($P < 0.001$). Hierarchical cluster analysis of this 974 gene set (*OATP1B3* gene signature) separated HCCs into two branches (B1 and B2) (Figure 1C). Thirty-four of the 36 *OATP1B3*-high HCCs (blue box) were classified in the left branch (B1), while *OATP1B3*-low HCCs were clustered in both branches.

The prognosis of HCC patients clustered in B1 was significantly better than those clustered in B2 ($P = 0.02$) (Figure S1). Genes associated with mature hepatocyte function such as *ALB* and *CYP3A4* were significantly up-regulated in the HCCs clustered in B1, and the known hepatic stem/progenitor markers *KRT19* and *EPCAM*, as well as the G1/S cell cycle marker *MKI67*, were significantly up-regulated in the HCCs clustered in B2 (Figure 1D).

Pathway analysis indicated that *OATP1B3*-high HCCs showed maintenance of mature hepatocyte function and decreased cell proliferation and Wnt signaling (Figure 1E), which are known to be activated during liver development and regeneration (15). Transcription factor analysis identified 8 genes (*HNF4A*, *NF1A*, *NR3C1*, *NR1I3*, *ESR1*, *NR1H3*, *MLXIPL*, and *NFE2L2*) as candidate transcription factors that were significantly activated in *OATP1B3*-high HCCs ($P < 0.005$) (Figure 1F). These transcription factors are known to play a pivotal role in liver development and in the regulation of hepatocyte functions including lipid, bile, carbohydrate, and xenobiotic metabolism (16). By contrast, only one gene (*FOXMI*) was identified as a candidate transcription factor activated in *OATP1B3*-low HCCs. The forkhead box M1 (FOXMI) transcription factor is known to be activated during liver regeneration and regulation of the cell cycle (17). We investigated the expression of the two transcription factors most strongly activated (*HNF4A* encoding hepatocyte nuclear factor 4 alpha [HNF4 α]) or inactivated (*FOXMI*) in hyper-intense HCCs (Figure S2) and validated the results using microarray analyses (Figure 2A, B).

Although the microarray data revealed distinct molecular portraits associated with liver development and the maturation programs present in hyper- and hypo-intense HCCs, hierarchical cluster analysis further indicated that a subset of hypo-intense HCCs (corresponding to the *OATP1B3*-low HCCs clustered in B1) might show similar gene expression profiles to those